Scalable Computing: Practice and Experience, ISSN 1895-1767, http://www.scpe.org

Volume 26, Issues 5, pp. 2070–2077, DOI 10.12694/scpe.v26i5.4911

INTERACTIVE DISPLAY SYSTEM INTEGRATING INFORMATION TECHNOLOGY IN ENVIRONMENTAL ART DESIGN

YUANYUAN YAO *AND ZHAOCHEN WANG †

Abstract. In order to solve the problems of dimensionality reduction and color display of spectral data after redundancy reduction in interactive display in environmental art design, the author proposes a research on an interactive display system that integrates information technology in environmental art design. The author first performs principal component transformation on the spectral data cube, assigning the first three components to the black and white channels, red and green channels, and yellow and blue channels in the color space. Then, after spatial transformation to sRGB space, the data is segmented and translated to the range of 0-1, mapped to 8-bit RGB, and single item evaluations of standard deviation, entropy, and average gradient are performed on each translated image. After all translations are completed, a comprehensive evaluation is performed on all evaluation values, and the interval with the highest comprehensive evaluation value is selected to output the mapping. The experimental results show that although this algorithm has a slightly longer time overhead, it is still far less than the acquisition time of 6.63 seconds for one spectral data cube, and is suitable for real-time detection applications of hyperspectral data. The fusion of images can maximize the energy, information, and clarity of the images, which is beneficial for the rapid recognition and judgment of the human eye.

Key words: Spectroscopy, Fusion display, Evaluation and selection, Environmental art design, Interactive Display

1. Introduction. With the development of the times, information technology has made rapid progress. Digital newspapers, online media, and self media platforms are all concrete manifestations of digital technology. Digital technology has accelerated the development speed of the design field, combining various advanced means such as computer technology and multimedia technology, subverting the traditional design ideas and paths, and making the previous environmental design methods more vivid and visual [1]. For example, digital images, 3D images, etc. are the result of combining traditional design methods with digital technology. In the digital age, the artistic nature of digital technology has become a new form and a key development trend in design and creation in the context of that era [2]. At the same time, the widespread application of digital technology has greatly improved the efficiency of environmental design. Environmental designers can also use various digital technological means to improve their creative efficiency, complete efficient creation of environmental art works, and enable all different forms of art to be combined with each other [3].

Environmental art and design is a comprehensive design discipline that integrates science and art into a theoretical system. The goal of environmental art design is to establish a sustainable humanistic and ecological environment, combine art and science for design, and better improve the human living environment. From the explanation of the concept of environmental art design at home and abroad, we can know that environmental art design is a systematic design project that includes multiple aspects, such as architectural design, garden design, urban community design, street design, public art design, public sculpture design, etc. It is a new discipline that includes art display and form display [4-6]. Environmental art design is a comprehensive art design process, to a certain extent, it is a holistic design that coordinates the relationship between humans and nature, and humans and society. This comprehensive design not only coordinates people's lifestyles, but also beautifies the natural environment, to a certain extent meeting people's spiritual needs and the need for harmonious coexistence between humans and nature. Modern interactive display design is a creative design activity that uses certain visual communication methods and exhibition facilities in the display space environment to display certain information and content in front of the public, and thus has a significant impact on the audience's psychology,

*College of Art and Design, Zhejiang Guangsha Vocational and Technical University of Construction, Jinhua, Dongyang, 322100, China.
†School of Economics and Management, Shangqiu Normal University, Shangqiu, Henan, 476000, China (Corresponding author, melody_wzc@163.com)

thoughts, and behavior. The author aims to explore how to effectively integrate information technology in environmental art design, construct innovative interactive display systems, and provide new ideas and practical guidance for the future development of environmental art design [7].

2. Literature Review. The fusion of imaging spectral data and pseudo color images in interactive display design of environmental art is one of the intuitive and effective ways to apply spectral data. The fusion processing provides pseudo color images that are easy for human eyes to observe and recognize. Spectral data fusion display first requires spectral data dimensionality reduction, and then the dimensionality reduction data is fused into a pseudo color image. The traditional dimensionality reduction data fusion method assigns the three images with the most information after dimensionality reduction to the RGB display model, which does not fully consider the characteristics of the dimensionality reduction data and the human eye's ability to distinguish different colors. Among all color spaces, the visual and psychological perception of color space and human eyes are relatively consistent [8]. Jiecheng, W. and others mainly analyze and explore the application of new media art in environmental art design to help us better understand the connotation of new media art [9]. Sang, Y. et al. introduced an algorithm called "Using Fuzzy Environmental Art Design" (EADF) to evaluate environmental standards and make better decisions. Initially, a fuzzy sequential preference technique similar to the Ideal Solution (FTOPSIS) was adopted in the design process, which considered multiple variables such as visual appeal, environmental impact, sustainability, and community audience engagement. Environmental art designers use the fuzzy TOPSIS method to evaluate artworks through multiple criteria [10]. Zhang et al. applied intelligent computer technology to environmental art design and combined it with intelligent computer technology to provide mathematical analysis tools required for precomputing light energy transmission technology. In addition, an environmental art design simulation system has been constructed. It is not difficult to see from the design evaluation results that the environmental art design system can effectively improve the effectiveness of environmental art design [11].

The author proposes a spectral data color fusion display algorithm based on multi interval translation mapping evaluation and optimization method to address the shortcomings of traditional pseudo color image display in environmental art interactive display design, which easily leads to mixed and difficult to distinguish targets. PCT dimension reduction data is allocated to the color space, and color data is mapped by inter partition translation for synchronous image evaluation. Finally, a comprehensive evaluation is conducted on all evaluation values, and the translation with the highest comprehensive evaluation is selected as the optimal translation [12]. The three optimal translation values are used to translate and map the color data of each channel, and the fused image with the best comprehensive energy, information, and clarity is obtained.

3. Method.

3.1. Principle of Hyperspectral Fusion Display. The spectral data cube undergoes redundancy reduction, noise reduction, and dimensionality reduction to obtain the dimensionality reduction data that best reflects the spectral features. It is then assigned to the corresponding color space and finally converted to the RGB space for storage and display. The principle is shown in Figure 3.1. The commonly used spectral data dimensionality reduction methods include band selection method, PCT method, independent component analysis (ICA), etc. Among them, PCT method has rigorous theoretical derivation, no iterative operation, and has received widespread attention. The author used PCT to achieve dimensionality reduction of spectral data.

The conversion of dimensionality reduction data to color space is the key to pseudo color display, which is related to whether the fusion result is consistent with human visual perception and whether the human eye can perceive various targets in the fusion result. The first three components of PCT are unrelated, with energy decreasing from strong to weak; The black and white channels O1, red and green channels O2, and yellow and blue channels O3 in the color space are also uncorrelated with the human eye, and their energy decreases from strong to weak. The first three components of PCT have similar characteristics to the color space of the human eye, and the three principal components of PCT can be assigned to 01, 02, and 03 [13,14]. It is not difficult to derive the conversion relationship from color space O1O2O3 to sRGB space based on the conversion

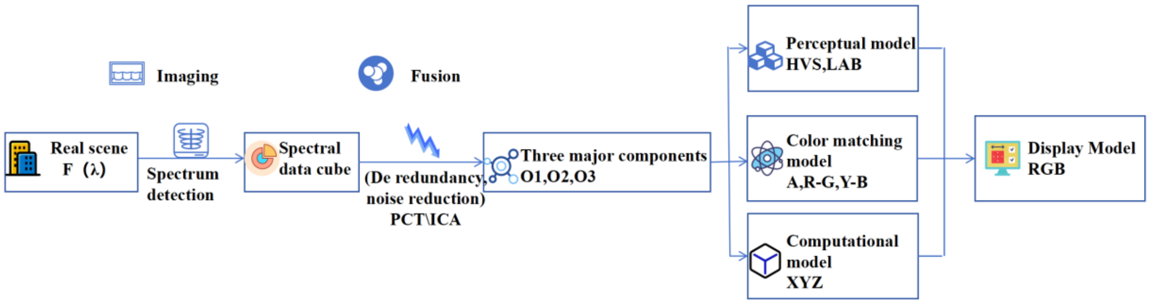

Fig. 3.1: Spectral imaging and fusion display process

relationship from color space to RGB image

$$[R_sG_sB_s] = \begin{bmatrix} 1.8063 & -5.8827 & -0.5766 \\ 0.6472 & 2.8929 & 0.1928 \\ 0.4103 & -0.0706 & 1.2418 \end{bmatrix} \begin{bmatrix} 01 \\ 02 \\ 03 \end{bmatrix} \tag{3.1}$$

Finally, a nonlinear transformation is performed to map the standard sRGB color space to an 8-bit RGB space, resulting in the final display result.

If $R_s, G_s, B_s \leqslant 0.00304$,

$$\begin{cases} R'_s = 12.92 \times R_s \\ G'_s = 12.92 \times G_s \\ B'_s = 12.92 \times B_s \end{cases} \tag{3.2}$$

If $R_s, G_s, B_s > 0.00304$,

$$\begin{cases} R'_s = 1.055 \times R_s^{1.0/2.4} - 0.055 \\ G'_s = 1.055 \times G_s^{1.0/2.4} - 0.055 \\ B'_s = 1.055 \times B_s^{1.0/2.4} - 0.055 \end{cases} \tag{3.3}$$

Finally, the non-linear $SR'G'B'$ value is converted into a digital encoded value according to the following equation:

$$\begin{cases} R_{8bit} = 255.0 \times R'_s \\ G_{8bit} = 255.0 \times G'_s \\ B_{8bit} = 255.0 \times B'_s \end{cases} \tag{3.4}$$

It is worth noting that in the above mapping process, only sRGB values within the [0,1] interval were captured, and values less than 0 and greater than 1 were not processed. This simple truncation mapping method sometimes cannot achieve the best visual display effect [15].

3.2. Multi information fusion translation mapping method. In order to map all values within the sRGB numerical range, a multi interval translation mapping method is used to map the sRGB standard color space to the RGB display space. That is, only a part of the sRGB numerical range is translated to the [0,1] interval each time, and the image quality after each translation mapping is comprehensively evaluated. Finally, the optimal interval of the image is selected for mapping. After transforming the color space 010203 to sRGB space, the minimum value of Rs is denoted as R_{min}, and the maximum value is denoted as R_{max} [16,17]. The translation formula is

$$\begin{cases} R_n = (R - R_{min}) - \Delta R \times i \\ i = 0 \sim N_R \\ M_R = [(R_{max} - R_{min})/\Delta R] + 1 \end{cases} \tag{3.5}$$

In the formula: R_n is the translated value; ΔR is the translation step size; N_R is the total number of translation steps; i is the step count value.

Record translation amount:

$$M = R_{min} + \Delta R \times i \tag{3.6}$$

Then there are:

$$R_n = R - M \tag{3.7}$$

When the step count value i is 0, R takes the value $[R_{min}, R_{min} + 1]$, corresponding to R_n taking the value [0,1]. Substitute R_s into equations 3.2 and 3.4 for nonlinear transformation mapping, which is equivalent to translating the values within the $[R_{min}, R_{min} + 1]$ range; When i is 1, the range of R values $[R_{min} + \Delta R, R_{min} + \delta R + 1]$ is mapped by translation; When i is 2, the range of R values $[R_{min} + 2\Delta R, R_{min} + 2\Delta R + 1]$ is mapped by translation; Translating all values within the R range sequentially will result in segmented translation mapping with δR as the translation step size [18]. After each translation mapping, a fused image will be obtained. After R_s translation, N_R images will be obtained. Similarly, after G_s, B_s translation, N_G, N_B images will be obtained. In total, $N_R \times N_G \times N_b$ pseudo color images will be obtained. If manual discrimination of image quality is used, it will require a lot of work. The author objectively evaluates each pseudo color image and finally selects the image with the highest evaluation value as the final fused result image [19].

3.3. Comprehensive evaluation of fused images. At present, there are many objective quality evaluation methods for fused images, including entropy based on image information, cross entropy, correlation entropy, joint entropy, mean, standard deviation, variance, and covariance based on image energy distribution, signal-to-noise ratio and peak signal-to-noise ratio based on image signal quality, and various evaluation methods based on clarity, average gradient, and spatial frequency. These individual evaluation methods generally focus on one aspect and do not have a comprehensive effect; Some evaluation methods are difficult to operate and are not suitable for evaluating fused images; Some evaluation results are inconsistent with the visual effects of the human eye.

The author proposes a comprehensive evaluation method of "evaluation, scoring, and synthesis". After each translation mapping, the standard deviation V_{std}, entropy value V_{ent}, and average gradient value V_{avg} are calculated separately. After all translation mappings are completed, the individual evaluation values are scored, denoted as:

$$y = E(x) \tag{3.8}$$

The range of evaluation values for different types varies, making it difficult to comprehensively evaluate. Therefore, it is necessary to "score" again. The author uses a sorting scoring method, where the minimum score for evaluation value is 1 and the maximum score is the number of evaluation values. Finally, conduct a comprehensive evaluation:

$$E = E(V_{std}) + E(V_{ent}) + E(V_{avg}) \tag{3.9}$$

Table 3.1 is a schematic table of the comprehensive evaluation method used. The comprehensive evaluation value E with a translation M of 1.0 in the table is the maximum value of 13. By substituting the translation M at this time into equation 3.7, the optimal fusion mapping result graph can be obtained [20].

Table 3.1: Schematic Table of Comprehensive Evaluation

Serial Number	Transla- -tion	standard deviation	entropy	average gradient	Standard deviation score	Entropy fraction	Gradient score	Comprehensive evaluation value
0	-2.0	80.4	0.70	30.4	1	2	1	4
1	-1.0	82.0	0.80	46.0	2	3	2	6
2	0.0	87.3	0.81	47.1	4	5	3	14
3	1.0	85.0	0.82	47.4	5	4	4	12
4	2.0	87.0	0.64	48.7	3	1	5	8

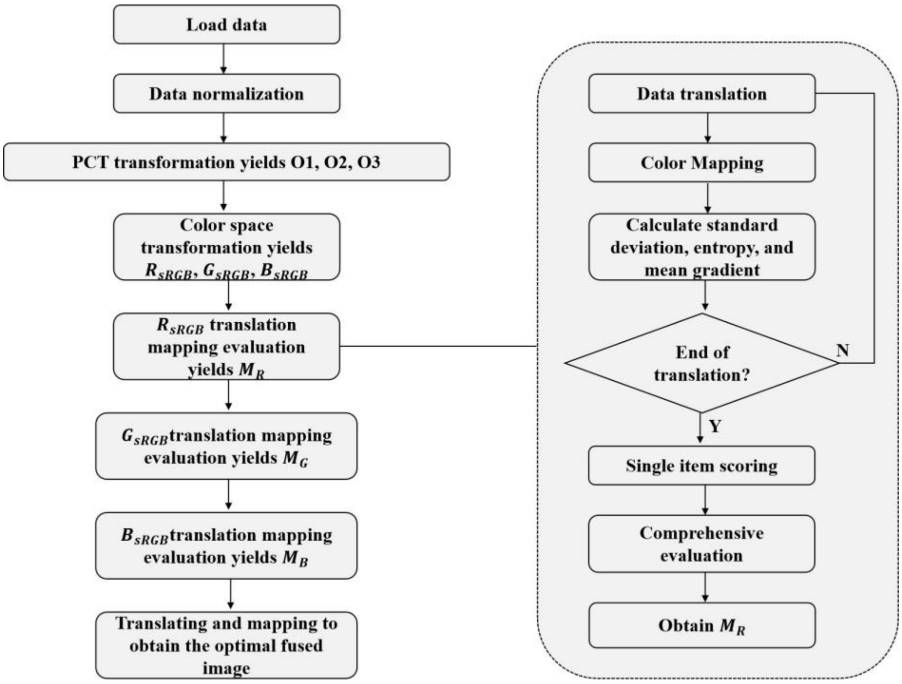

Fig. 3.2: Algorithm flowchart

3.4. Algorithm Implementation. The algorithm implementation process is shown in Figure 3.2. The specific implementation process is as follows:

1) Initialization: Set the translation step size $\Delta R = 0.5$, load hyperspectral data, and normalize it;
2) Spectral data dimensionality reduction: Perform principal component transformation on hyperspectral data to obtain the first three principal components after transformation;
3) Spatial variation: Assign the first principal component after PCT to the black and white channel 01 in the color space, assign the second principal component to the red and green channel 02 in the color space, and assign the third principal component to the yellow and blue channel 03 in the color space. Transform the color space data into sRGB space using equation 3.1 to obtain R_s, G_s, B_s;
4) Evaluate the translation mapping of the red component and obtain the optimal translation amount M_R for the red component; Use equation 3.5 to translate R_s, and after each translation, use equations 3.2 and 3.4 for mapping, and perform single item evaluations of standard deviation, entropy, and average gradient; After the translation is completed, use equations 3.8 and 3.9 for individual scoring and comprehensive evaluation, and obtain the red component translation amount M_R when the image quality is optimal through the optimal evaluation value E_R;
5) Green component translation mapping evaluation, obtaining the optimal translation amount for the green

Table 4.1: Performance Comparison of Four Mapping Methods

Mapping display method	R standard deviation	R entropy	R gradient	G standard deviation	G entropy	G gradient	B standard deviation	B entropy	B gradient
T. A. 2000	24.535	6.435	10.163	45.722	7.036	14.341	18.045	6.043	8. 875
J. S. T. 2003	47.432	7. 102	15.437	40.216	7. 002	16.166	30.071	6.627	10.702
Simple excerpt	92.027	1.027	16. 065	79.038	5.763	33.801	56.100	1. 601	4.8464
Author's Algorithm	113. 145	4.086	44.743	106.881	4.528	43.560	73.064	6.676	35.274

component, using the same method as step 4);

6) Evaluate the blue component translation mapping to obtain the optimal translation amount M_B for the blue component, using the same method as step 4);
7) Optimal image fusion mapping: Substitute M_R, M_G, and M_B into equation 3.7 to obtain translated R_s, G_s, and B_s; map the optimal fusion image using equations 3.2 and 3.4.

3.5. Experimental verification. The experimental equipment adopts a self-developed visible light imaging spectrometer, with a band range of $0.4\mu m \sim 0.9\mu m$, spatial resolution of 491 pixels (h) $\times$ 674 pixels (w), and a narrowband count of 61. The experimental subjects are 6 different $500mm \times 500mm$ camouflage target fabrics, with clear weather and an experimental distance of 100m; The collected spectral data cube is normalized and transformed by PCT.

4. Results and Discussion. In order to verify the author's fusion display algorithm, the author chose to compare it with Tirance Achalakul's color space mapping method proposed in 2000, J. Scott Tyo's HSV mapping method proposed in 2003, and a simple [0,1] interval mapping method. Table 4.1 is a comparison table of evaluation values for camouflage target plates.

A.2000 and J S. The two mapping methods of T.2003 have a soft overall color tone and can display the information content of all scenes in a summarized manner, but the contrast of the image is low and the details of the camouflage target board are difficult for the human eye to distinguish; Simple cropping and this algorithm have high image contrast and strong contrast between light and dark, reflecting the characteristics of the cropping mapping method; The simple truncation method only directly maps the [0,1] interval, but the information content of this part is not optimal and loses the details of the camouflage target; The algorithm used by the author traverses all possible values, selects the best among them, and the resulting image best reflects the details of the image. From the evaluation values of the camouflage target board in Table 4.1, it can be seen that compared to other methods, the evaluation values of this algorithm are significantly superior except for a slight decrease in entropy, indicating that the contrast and clarity of this algorithm are significantly better than other methods. T.Although the information content of the image is reduced, the human eye is more likely to distinguish the details of the camouflage target, which is consistent with the visual recognition effect of the human eye.

Table 4.2 lists the runtime models and testing times for four different schemes, where T_1 represents the PCA runtime; T_2 represents spatial transformation time; T_3 represents the digital image transformation time; T_4 represents the color space transformation time; T_5 represents the time of data interception; T_6 represents the translation mapping time. stay i5-3470@3.20GHz On a quad core CPU computer, the MatlabR2007a software platform was used to test the running time of four methods. As shown in Table 4.2, the running time of the first three methods is almost the same. Although this algorithm has a slightly longer time overhead, it is still far less than the acquisition time of one spectral data cube, which is 6.63s. It is suitable for real-time detection applications of hyperspectral data.

Table 4.3 lists the comprehensive evaluation values during the program running process. It can be seen from Table 4.3 that the comprehensive evaluation value is highest when the R channel translation step is 7, and the optimal translation amount for mapping the image is -4.1021.

(5) The ΔR translation step size of the equation affects the final mapping result. It is worth noting that when the translation step size is 1, there is no overlap in the translation intervals. When the translation step

Table 4.2: Comparison of Running Times for Four Mapping Methods

Mapping display method	Calculate time model	run time/s
T. A. 2000	T1+T2+T3	1.021
J. S. T. 2003	T1+T2+T3	1.01
Simple excerpt	T1+T4+T5+T3	1.037
Author's Algorithm	T1+T4+T6+T3	1.608

Table 4.3: Schematic Table of Comprehensive Evaluation of R Channel Part

Serial Number	Transla--tion	standard deviation	entropy	average gradient	Standard deviation score	Entropy fraction	Gradient score	Comprehensive evaluation value
4.0	-5.501	41.665	1.040	16.022	16.0	20.0	17.0	54.0
5.0	-5.001	77.563	3.040	34.407	18.0	26.0	26.0	72.0
6.0	-4.501	104.033	4. 213	45.853	24.0	31.0	31.0	84.0
7.0	-4.001	113.145	4.086	44.743	31.0	28.0	28.0	87.0
8.0	-3.501	112.220	3.018	37.031	28.0	27.0	27.0	84.0
9.0	-3.001	109.407	2.015	28.251	27.0	25.0	25.0	80.0
10.0	-2.501	107.063	1.382	22.604	23.0	24.0	24.0	76.0
...	...	...	...	...	...	...	...	...

Table 4.4: Performance Comparison of Different Translation Steps

Translation step size	thorough--fare	Serial Number	Transla--tion	standard deviation	entropy	average gradient
	R	4.0	-3.501	112.220	3.018	37.031
1	G	6.0	-0.301	106.881	4.528	43.560
	B	4.0	-0.386	68.303	5.568	17.252
0.8	R	4.0	-4.301	109.512	4.266	46.406
	G	7.0	-0.701	99.321	3.367	40.200
	B	5.0	-0.386	68.303	5.568	17.205
0.5	R	7.0	-4.001	113.145	4.086	44.743
	G	12.0	-0.301	106.881	4.528	43.561
	B	7.0	-0.886	73.064	6.676	35.274
	R	11.0	-4.201	111.222	4.232	46.207
0.3	G	20.0	-0.301	106.881	4.528	43.560
	B	12.0	-0.786	72.057	6.761	31.747

size is less than 1, there is overlap in the translation intervals. The smaller the translation step size, the more overlapping areas there are. However, this overlapping translation is indeed beneficial, because when converting the value of to RGB [0.255], grayscale values close to 0 and 255 are insensitive to human eye discrimination and recognition. When the translation step is 1, some optimal images will be lost. In theory, the smaller the translation step, the better, but this will cause a sharp increase in computational complexity. Table 4.4 presents a performance comparison table for different translation steps, and the numerical evaluation results are basically consistent with the human eye evaluation results.

5. Conclusion. The author proposes a research on an interactive display system that integrates information technology in environmental art design. Spectral data fusion and color display are key factors for real-time application of hyperspectral imaging sensors in environmental art interactive display design. The spectral data color fusion display algorithm proposed by the author ensures that the final mapped image quality is optimal within a selectable range through segmented translation, mapping, evaluation, and optimization methods. Not only does it avoid the disadvantage of directly capturing the 0-1 part of color data, but it also avoids the problem that digital mapping can easily result in low-energy targets less than 0 and high-energy targets greater than 1 being unable to be distinguished and displayed in the fused image; It also solves the problem of overall compression of color data to the 0-1 range, resulting in low contrast in digital mapping images and difficulty in distinguishing details with the human eye. The experimental results show that the algorithm can significantly improve the energy and clarity of the fused image, with high contrast and clear distinction of details, which is conducive to rapid recognition and judgment by the human eye. The algorithm principle is simple and easy to implement, and has broad application prospects in real-time reconnaissance of hyperspectral imaging sensors.

REFERENCES

[1] Yu, Y., & Yu, D. (2023). Research on the visual media design system of brands integrating new media technology in the attention economy. Proceedings of the 2nd International Conference on Information, Control and Automation, ICICA 2022, December 2-4, 2022, Chongqing, China.

[2] Li, B., & Lu, W. (2024). Application of image processing technology in the digital media era in the design of integrated materials painting in installation art. Multimedia Tools and Applications, 83(18), 54211-54228.

[3] Derkach, S., Melnyk, M., Fisher, V., Krypchuk, M., & Sovhyra, T. (2023). Video mapping technologies as spatial augmented reality in the artistic process. Preservation, Digital Technology And Culture, 52(2), 59-68.

[4] Chen, Y. (2023). The path and value of integrating ecological aesthetic education into the teaching of environmental art design major. Journal of Contemporary Educational Research, 7(11), 190-196.

[5] Liao, X. (2024). Protecting the environment through art: the significance of environmental art design in raising awareness about environmental pollution among universities in china. Current Psychology, 43(32), 26548-26570.

[6] Sullivan, A., Gianotti, A. S., Scollins, A., Tornatore, L., Ge, B., & Briones, M. (2024). Undergraduate experiences with sustainability courses: insights for diversifying sustainability education. Journal of Environmental Studies and Sciences, 14(3), 548-567.

[7] He, J., & Wu, Y. (2022). Application of digital interactive display design based on computer technology in vr film. Mobile information systems, 2022(Pt.31), 1-7.

[8] Zheng, Y. (2023). The generalized dice similarity measures for comprehensive evaluation of graphic design effects based on color psychology with t-spherical fuzzy sets. Journal of Intelligent & Fuzzy Systems: Applications in Engineering and Technology, 45(4), 6413-6427.

[9] Jiecheng, W. (2023). Analyze the application of new media technology in environmental art design. Procedia Computer Science, 228, 907-913.

[10] Sang, Y. (2024). Application in environmental art design practice based on a fuzzy evaluation system. Scientific Reports, 14(1).

[11] Zhang, H. (2024). Intelligent computer technology and its application in environmental art design. International Journal of Information and Communication Technology, 24(2), 213-227.

[12] Grzelec, M. (2024). Application of attenuated total reflectance—fourier transform infrared spectroscopy—(atr-ftir) and principal component analysis (pca) in identification of copying pencils on different paper substrates. Heritage Science, 12(1), 1-16.

[13] Shang, H., Li, P., & Peng, X. (2024). Enhancing the quality of low-light printed circuit board images through hue, saturation, and value channel processing and improved multi-scale retinex. Journal of Computer and Communications, 12(1), 1-10.

[14] Gan, Y., Zhang, H., & Yi, C. (2024). Multiscale fusion transformer network for hyperspectral image classification. JOURNAL OF BEIJING INSTITUTE OF TECHNOLOGY, 33(3), 255.

[15] Falahatnejad, S., & Karami, A. (2023). Deep fusion of hyperspectral and lidar images using attention-based cnn. SN Computer Science, 4(1), 1-11.

[16] Tian, X., Zhang, W., Yu, D., & Ma, J. (2023). Sparse tensor prior for hyperspectral,multispectral,and panchromatic image fusion, 10(1), 284-286.

[17] Zhang, Y., Zhang, J., Xu, S., & Yang, L. (2024). Research on fracture prediction method based on multi-source information fusion. Journal of Geoscience and Environment Protection, 12(6), 14.

[18] Tange, R. (2023). A combinatorial translation principle and diagram combinatorics for the general linear group. Transformation groups, 28(4), 1687-1719.

[19] Han, Y., Lu, G., Zhang, S., Zhang, L., Zou, C., & Wen, G. (2024). A temporal knowledge graph embedding model based on variable translation. Tsinghua Science and Technology, 29(5), 1554-1565.

[20] Hung, B. T., & Thu, N. H. M. (2024). Novelty fused image and text models based on deep neural network and transformer for multimodal sentiment analysis. Multimedia Tools and Applications, 83(25), 66263-66281.

Edited by: Hailong Li
Special issue on: Deep Learning in Healthcare
Received: Sep 13, 2024
Accepted: Oct 21, 2024